

On the stability of fractal globules

Raoul D. Schram,^{1,a)} Gerard T. Barkema,^{1,2,b)} and Helmut Schiessel^{1,c)}

¹*Instituut-Lorentz, Leiden University, P.O. Box 9506, 2300 RA Leiden, The Netherlands*

²*Institute for Theoretical Physics, Utrecht University, P.O. Box 80195, 3508 TD Utrecht, The Netherlands*

(Received 11 March 2013; accepted 3 May 2013; published online 10 June 2013)

The fractal globule, a self-similar compact polymer conformation where the chain is spatially segregated on all length scales, has been proposed to result from a sudden polymer collapse. This state has gained renewed interest as one of the prime candidates for the non-entangled states of DNA molecules inside cell nuclei. Here, we present Monte Carlo simulations of collapsing polymers. We find through studying polymers of lengths between 500 and 8000 that a chain collapses into a globule, which is neither fractal, nor as entangled as an equilibrium globule. To demonstrate that the non-fractalness of the conformation is not just the result of the collapse dynamics, we study in addition the dynamics of polymers that start from fractal globule configurations. Also in this case the chain moves quickly to the weakly entangled globule where the polymer is well mixed. After a much longer time the chain entangles reach its equilibrium conformation, the molten globule. We find that the fractal globule is a highly unstable conformation that only exists in the presence of extra constraints such as cross-links. © 2013 AIP Publishing LLC. [<http://dx.doi.org/10.1063/1.4807723>]

I. INTRODUCTION

Progress in experimental methods to study the conformation of DNA *in situ* has recently revived the interest in various only partially understood polymer physics problems. The fractal globule plays a prominent role here. It has been suggested¹ that this non-equilibrium polymer configuration is brought about by the sudden collapse of a long polymer in a Θ or good solvent when one switches the system suddenly to poor solvent conditions. As the polymer crumbles at successively larger and larger length scales, a self-similar fractal of fractal dimension 3 ensues where the chain is segregated on every length scale. The non-mixing of the subchains was based on an argument¹ where the subchains were compared to polymer rings who are known not to mix.^{2,3} Only through a much slower process involving the chain ends the polymer reaches eventually its equilibrium state, the molten globule.

A hallmark of the fractal globule is that it is non-entangled. Switching back to good solvent conditions, a fractal globule grows quickly back into a swollen coil. This is radically different for a molten globule that is highly entangled and thus gets arrested during swelling. Grosberg *et al.*¹ suggested that the fractal globule conformation might share common features with the conformations of biological macromolecules such as DNA and proteins. Especially for eukaryotic DNA that can have lengths of centimeters, fractal conformations could be crucial as the genome might be otherwise inaccessible due to the entanglements.⁴

For a long time it has been difficult to test this idea experimentally. One way to detect the conformation is to measure the spatial distance $r(g)$ between two monomers as a function of the chemical distance $g = |i - j|$ (the genomic distance for DNA). Such measurements have indeed been

performed for eukaryotic chromosomes since a long time through the use of fluorescence in situ hybridization (or FISH for short).⁵⁻⁷ However, it is very hard if not impossible to extract an exponent from the data, especially due to large cell-to-cell variations.⁸

A new molecular biology technique called chromosome conformation capture promises to shed light on the problem. This method allows for measuring, genome wide, the contact probability p_c between DNA segments as a function of their genomic distance g . The contact probability is defined as the probability that two monomers at a genomic distance g are equal or less than an Euclidean distance R_0 apart. Chromosome conformation capture of human lymphoblasts produced approximately $p_c \sim g^{-1}$ in the range from 500 kbp to 7 Mbp (bp: basepair).⁹ The -1 slope does not occur for standard polymer models which raises the question whether it could be found for fractal globule configurations. The authors of Ref. 9 claim that this is indeed the case. They distinguish two types of fractal globules, smooth and interdigitating ones. Smooth fractal globules lead to the slope $-4/3$ in the contact probability whereas interdigitating fractals have the “proper” slope of -1 .¹⁰ An important note to make here is that the relation between the exponent characterizing the decay and the polymer conformation (here -1 and the interdigitating fractal globule) is not a one-to-one relation. Thus, any proposed structure must preferably make predictions of other experimentally measurable quantities, before one can conclude for certain whether this conformation matches the DNA in the cell nucleus. Nevertheless, Liebermann-Aiden *et al.*⁹ showed through Monte Carlo simulations that their procedure of rapidly collapsing a polymer from its swollen state leads to a conformation that has a -1 slope and which is claimed to resemble the interdigitating fractal globule.

Through Monte Carlo simulations we show that the collapse of a swollen polymer coil through a change in solvent does not reproduce the -1 slope. Even though polymer

^{a)}Electronic mail: schram@lorentz.leidenuniv.nl

^{b)}Electronic mail: g.t.barkema@uu.nl

^{c)}Electronic mail: schiessel@lorentz.leidenuniv.nl

collapse occurs in a hierarchical fashion, as predicted in Ref. 1 and observed, e.g., in Refs. 11 and 12, the subchains mix so quickly that the polymer directly after the collapse is at first sight nearly indistinguishable from an equilibrium globule. In particular, we find for $g < N^{2/3}$ the relations $r(g) \sim g^{1/2}$ and $p_c \sim g^{-3/2}$, each supposedly a hallmark of the molten globule. Such a polymer is, however, not yet in equilibrium as it is nearly as little entangled as it was in its original swollen coil conformation. Only via a much slower mechanism the equilibrium is finally reached.

Inspired by this result, we started to question the stability of the fractal globule itself. To this effect we prepared fractal conformations by hand and studied their consecutive relaxation to the equilibrium structures. The considered fractals have the above mentioned properties that subchains are spatially separated and that the whole chain is “unentangled.” We found that such structures are not stable but that the chain mixes quickly on all length scales in less than N^2 time steps, producing an unentangled pseudo-equilibrium globule before the global equilibrium is reached via a much slower process.

Thus, to maintain the notion of a fractal globule as the structure of DNA in the cell nucleus, one has to show either one of three things: either even the longest polymers that we can simulate (8000) are too short to capture the asymptotic behavior, or the time scale of the cell cycle is extremely short from a polymeric point of view, or other “ingredients” are present to maintain the structure of the globule. One such “ingredient” could be the addition of cross-links, see, e.g., Ref. 13. In this paper we approach the problem instead from a polymeric point of view, since we are of the opinion that with our current knowledge of chromatin structure the latter two approaches are at least highly debatable.

The remainder of the paper is divided into three sections. First in Sec. II the Monte Carlo method and the fractal starting conformations are described in detail. In Sec. III we give a theoretical background on the problem of fractal globules and present the results of the Monte Carlo simulations. In Sec. IV we attempt to piece the whole story together.

II. MONTE CARLO METHOD

A. Basis implementation

Our Monte Carlo simulation method uses a lattice polymer model that is based on Rubinsteins repton model.¹⁴ For other applications see, e.g., Refs. 15 and 16. The monomers of the polymer lie on an underlying lattice. The choice of lattice in three-dimensional space is usually limited to the simple cubic (SC), body-centered cubic (BCC), and face-centered cubic (FCC) lattices, because of the translation symmetry of points on the lattice, with each point of the lattice being equivalent. We use the FCC lattice as the underlying lattice of the simulations. One advantage of this lattice is that moving from one point of the lattice to another can be made in an arbitrary number of steps, which improves the possibilities to find valid Monte Carlo moves. On the SC and BCC lattices this is not the case, because the number of steps to go from one point to another is always either even or odd. The polymer consists of N monomers where consecutive monomers are either on ad-

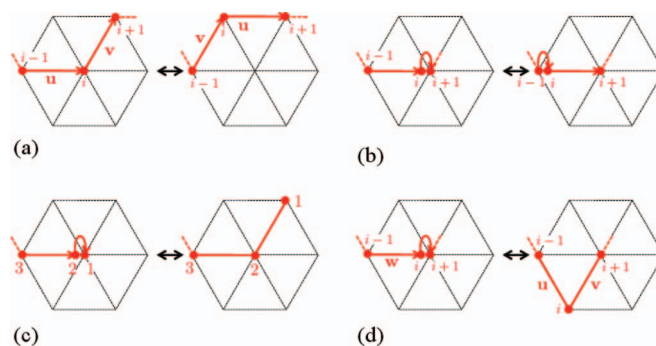


FIG. 1. Schematic depiction of the Monte Carlo moves. The arrows denote the bond vectors, where an arrow that ends and starts at the same monomer is an element of stored length. (a) and (b) Instances of corner moves. (c) The end moves. (d) An example of a transversal move.

jacent points on the lattice or on the same lattice site. We call the bond between two consecutive monomers on the same site a unit of “stored length.” We allow stored length, because it speeds up the simulation, even though the effective length of the polymer is slightly smaller (by a constant fraction). Only consecutive monomers are allowed to occupy the same site. Thus there is still excluded volume interaction between the monomers.

The dynamic properties of the Monte Carlo method is governed by its “moves.” At each Monte Carlo step a monomer is selected at random and one Monte Carlo move is attempted on the monomer. Independent of the success of this move, the time in the Monte Carlo simulation is increased by $1/N$. Thus after N Monte Carlo moves the time has increased by one unit of time. The Monte Carlo moves involve manipulations of the vectors between two consecutive monomers, the bond vectors, that can either have the length 0 (in case of stored length) or 1 (for monomers at neighboring lattice sites). The basic moves of our Monte Carlo algorithm are depicted in Fig. 1 and are defined as follows:

- Corner move: Select an inner monomer i and interchange the two bond vectors \mathbf{u} and \mathbf{v} , where $\mathbf{u} = \mathbf{r}_{i+1} - \mathbf{r}_i$ and $\mathbf{v} = \mathbf{r}_i - \mathbf{r}_{i-1}$. For example, the tuple (\mathbf{u}, \mathbf{v}) would transition to (\mathbf{v}, \mathbf{u}) after the move. If one of the bond vectors \mathbf{u} and \mathbf{v} has zero length, the corner move effectively diffuses stored length along the polymer chain.
- Forward end move: Select one end. If the end has stored length, then extend the monomer to a random site around the position of the end monomer.
- Backward end move: Reverse of the forward end move.
- Forward transversal move: If the bond vectors adjacent to the selected monomer are either of the form $(0, \mathbf{w})$ or $(\mathbf{w}, 0)$, move it to a tuple (\mathbf{u}, \mathbf{v}) , with $\mathbf{w} = \mathbf{u} + \mathbf{v}$.
- Backward transversal move: Reverse of forward transversal move.

Moves that violate the self-avoidance constraint are always rejected. Only moves are allowed that move a monomer over exactly one unit distance. The chemical potential between stored length and non-stored length can be adjusted

through the acceptance rate of the moves. In our simulations we chose a 1:2 acceptance ratio between stored length and non-stored length. This implies a 1:1 ratio for the backward/forward transversal moves, because a tuple $(0, \mathbf{w})$ has on the FCC lattice 4 different tuples (\mathbf{u}, \mathbf{v}) , that move the monomer over distance 1. The reverse move has two possibilities: $(0, \mathbf{w})$ and $(\mathbf{w}, 0)$. The forward end move has 12 possibilities (although one of them will always be rejected). The backward move has only one possibility, and thus the acceptance ratio is 1:6 between the forward and backward moves. This ensures detailed balance. It is easy to see that the ergodicity condition is also satisfied, because it is possible to completely retract the polymer to a single point, and from there with corner moves and forward end moves all possible configurations can be created.

B. Self-attraction

Self-attraction of the polymer is accomplished by favoring moves, that decrease the surface of the polymer. More formally, in our model we define the Hamiltonian as follows:

$$H = \mu \sum_{0 \leq i < N} s_i - \epsilon \sum_{i,j} p_{ij}. \quad (1)$$

Here s_i is one if a bond vector is stored length, and zero otherwise. p_{ij} is one if monomers i and j are next to each other, otherwise zero. If through stored length more than one monomer occupies a site, only one monomer is counted in the sum for p_{ij} . This is done to keep stored length from accumulating next to each other. The acceptance ratios of all moves are adjusted to maintain detailed balance. In the following we choose $\mu = 0.25$ and $\epsilon = 0.25$. The s_i term is introduced, because otherwise the stored length ratio would change significantly from the case without self-attraction, and also would strongly depend on the actual shape of the globule. There are only a limited number of transitions in energy, because sums in the Hamiltonian are integers. Therefore, we store all the possible acceptance rates in a small table for efficiency. In our simulations the amount of stored length varies between 11% and 13%.

C. Chain crossing

In some of our simulations we allow chain crossing. The chain crossing move is a special variant of the corner move. If we allow chain crossing, then if the corner flip is rejected by a self-avoidance constraint, we also try to move the monomer that blocks the original move by the means of a corner move. We accept the combination corner move, if the monomers are interchanged by the moves. The Hamiltonian of the self-attraction does not change with such a move, and therefore the chain crossing move does not need to take it into account. This extra move adds a small factor to the simulation time, but on the other hand, the overall dynamics of the polymer are sped up substantially.

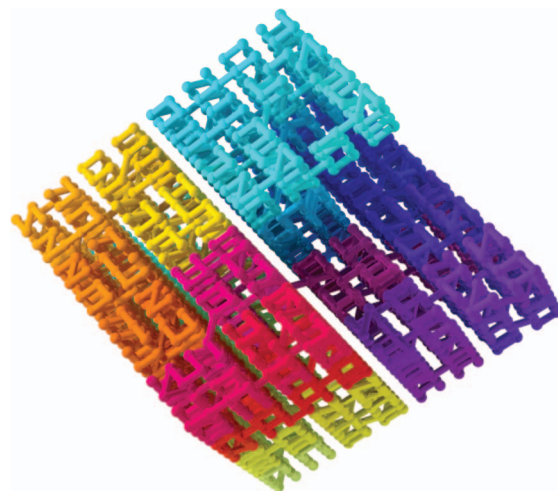


FIG. 2. A sample random FCC fractal of length $N = 4000$.

D. Random FCC fractal

For the simulation of the equilibration of a smooth fractal globule, we introduced a space filling randomized fractal creation method specifically designed for the FCC lattice, see Fig. 2 for an example. Another option would have been using a standard method for creating Hilbert or Peano curves, but we found that our method creates smoother contact probability curves than non-random versions of the aforementioned curves.

The shape of the FCC fractal is a $L \times L \times L$ parallelepiped which is described by the non-orthogonal basis: $\mathbf{t} = (1, 1, 0)/\sqrt{2}$, $\mathbf{u} = (1, -1, 0)/\sqrt{2}$, $\mathbf{v} = (-1, 0, 1)/\sqrt{2}$. Note that $\{\mathbf{t}, \mathbf{u}, \mathbf{v}\}$ is almost an orthogonal basis, and thus the shape of the parallelepiped is close to cubic. In the first iteration, this cube has size $2 \times 2 \times 2$, and one of the possible self-avoiding walks is chosen that is visiting all points in this cube with length 7 (and thus 8 monomers). In further iterations each monomer is chosen as a seed for another $2 \times 2 \times 2$ cube. Care has to be taken to ensure that links on the new $2 \times 2 \times 2$ cubes interconnect. Depending on their relative position, two cubes can have a different number of possible interconnects. If two cubes are separated by a plane, the number of points facing each other on each side is equal to 4. The two other possibilities are separated by a line (diagonal in one direction, 2 points), and separated by a point (diagonal in two directions, 1 point). By first setting the interconnects that are the most urgent (least number of possible interconnects), conflicts are avoided to the maximum extent. No problematic conflict was ever detected using our prioritizing, even with the fractal of $N > 10^8$, suggesting that this is in fact theoretically impossible. A proof, however, is beyond the scope of this article. If more than one interconnect is possible, the interconnect is chosen randomly.

When the interconnects are determined, one of the still possible self-avoiding walks inside the $2 \times 2 \times 2$ cube is randomly selected for each cube. The advantage of the FCC lattice here is that for every possible combination of in and outgoing interconnects, there is always at least one possible

space filling self-avoiding walk in the $2 \times 2 \times 2$ cube connecting them.

III. RESULTS

In this section we present results from our Monte Carlo simulation. We start by setting up the necessary theoretical background to interpret the results in Subsection III A. In Subsection III B we study polymer collapse focusing on the state immediately after the collapse. To learn more about this state we study next the dynamics of fractal globule with chain crossing, Subsection III C, and without chain crossing, Subsection III D.

A. Theoretical preliminaries

Though the contact probabilities for both the interdigitating and smooth fractal globule have already been derived in Ref. 9, we present here a shorter, more intuitive derivation.

For an equilibrium molten globule of polymerization degree N one expects $r(g) \sim g^{1/2}$ (as long as this distance is smaller than the overall globule size, i.e., as long as $g < N^{2/3}$) as the result of the screening of the excluded volume.^{8,17} On the other hand, a fractal globule of fractal dimension 3 would simply give $r(g) \sim g^{1/3}$ for any value of g .

For a molten globule the polymer is mixed on all length scales. Two monomers at a distance g apart are connected by a subchain that takes up a volume proportional to $g^{3/2}$. The contact probability $p_c = p_c(g)$ is then simply inversely proportional to that volume, $p_c \sim g^{-3/2}$. If one would recycle this argument for the fractal globule (which is not allowed as the chain is not mixed), one would predict $p_c \sim g^{-1}$.

There are deterministic counterparts to fractal globules, space-filling curves like the three-dimensional Peano and Hilbert curves. The problem with the simple argument above is that it does not account for the fact that the chain is demixed on all length scales. This means, for instance, that if we look at a chain section of length g , its two $g/2$ monomers long subchains (each taking up a volume $v \sim g$) will not mix. From this follows that two monomers a genomic distance g apart can only be in contact if both monomers reside on the interface between the two subchains (each with probability $v^{2/3}/v \sim g^{-1/3}$) and that they meet then on this interface (additional factor $1/v^{2/3} \sim g^{-2/3}$). In total the contact probability of the fractal globule should obey $p_c \sim g^{-1/3} \times g^{-1/3} \times g^{-2/3} = g^{-4/3}$, in agreement with the finding for the above mentioned deterministic curves.

Now, let us widen our definition of the fractal globule by releasing the constraint that it has to be “smooth.” Instead, the interface between the two $g/2$ monomer long subchains is a fractal surface with fractal dimension $2 \leq d_s \leq 3$. Now the probability for a monomer to be at the fractal surface of its subchain is $v^{d_s/3}/v \sim g^{d_s/3-1}$ and the probability that two given interface monomers are in contact is proportional to $v^{-d_s/3} \sim g^{-d_s/3}$. Altogether this leads to a contact probability that scales like $p_c \sim g^{d_s/3-1} \times g^{d_s/3-1} \times g^{-d_s/3} = g^{d_s/3-2}$, see also Ref. 2. For a smooth interface, $d_s = 2$, we recover the relation $p_c \sim g^{-4/3}$. In general the exponent can vary be-

tween that value and the value -1 for $d_s = 3$. It is that latter case that the authors of Ref. 9 refer to as interdigitated fractal. In that case the interface has the dimension of a volume and different subchains overlap. To ensure self-similarity the thickness of the overlapping zone has to scale with the volume of the subchain as $v^{-1/3}$.

A more refined argument is given in the Appendix.

B. Collapse of a polymer in a poor solvent

It was proposed in Ref. 1 that a polymer directly after a collapse – as induced by a change in the solvent quality from good to poor – is temporarily trapped in the fractal globule state. According to the simulation presented in Ref. 9 that state is of the interdigitating type. The main argument for the existence of such a metastable state is based on the idea that the equilibration of a fractal globule is achieved by reptation which is a slow process—at least of the order N^3 . The collapse of a polymer happens on an asymptotically much shorter time scale, namely, $O(N^{1+2\nu})$ with $1 + 2\nu \approx 2.2$ for a swollen chain through Rouse dynamics.¹⁸ The latter neglects hydrodynamic interactions that would make this process even faster.

We present here simulations of the collapse of a polymer induced by a sudden change in solvent quality from good to poor. The polymer has a length $N = 4000$. The starting configuration is that of a swollen coil which results from the excluded volume that is built into the model as outlined in Sec. II. When switching on the self-attraction the polymer crumples in a hierarchical fashion as originally proposed in Ref. 1 and already observed in computer simulations.^{11,12} Despite this we find that the state momentarily after the collapse of the polymer does not resemble that of a fractal globule. In our simulations, we take for the cutoff radius of the contact probability R_0 one lattice distance. As seen in Figs. 3 and 4, the $r^2(g)$ and $p_c(g)$ plots of the collapsed polymer resemble closely the ones expected for an equilibrium globule,

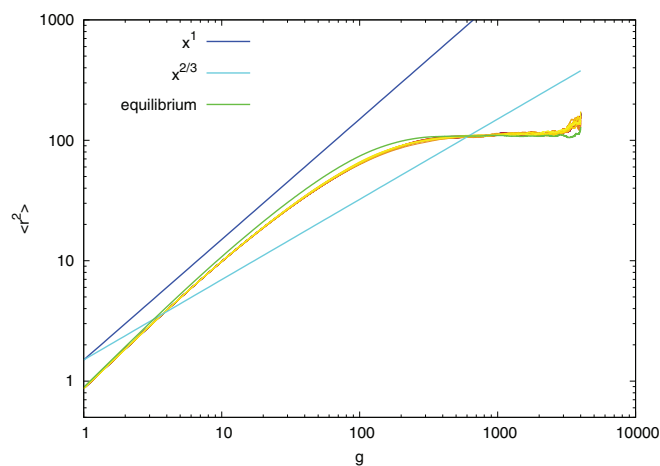


FIG. 3. Polymer of length $N = 4000$ in a poor solvent, directly after the collapse from a swollen coil. Chain crossing is not allowed in this simulation. Depicted is the mean squared monomer-monomer distance versus the distance g along the chain. The time starts with the black curve just after the polymer reaches the globular state. This curve is hidden under the sequence of curves up to the yellow curve N^2 time steps later. All these curves can clearly be distinguished from the molten globule equilibrium curve (green).

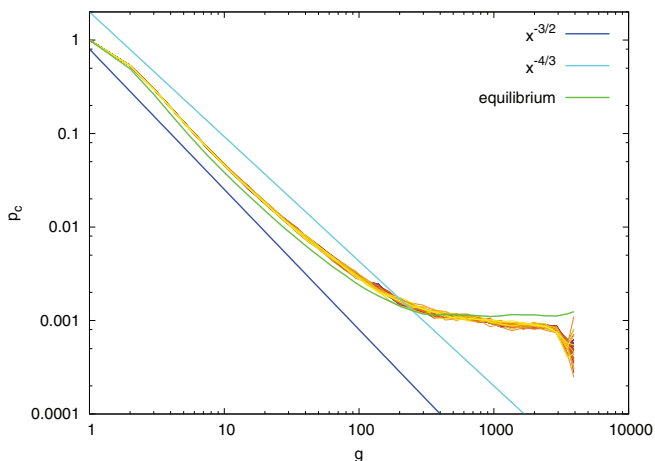


FIG. 4. The contact probability $p_c(g)$ is plotted against the distance along the chain. Everything else is the same as in Fig. 3.

namely, $r^2 \sim g$ and $p_c \sim g^{-3/2}$. This is in clear contrast to the relations $r^2 \sim g^{2/3}$ and $p_c \sim g^{-1}$ that have been reported in Ref. 9 for a collapsed chain of similar length. Since the collapse in our simulations takes approximately $N^{1+2\nu}$ units of time, we do not expect that this polymer configuration corresponds to an equilibrium globule since the polymer would need a time $O(N^3)$ to entangle itself completely.

Remarkably the plots of $r(g)$ and $p_c(g)$ shown in Figs. 3 and 4 do not change noticeably over a span of N^2 time steps as curves for different times lie on top of each other. The system has, however, not reached equilibrium. To demonstrate this we plot in these figures also the equilibrium curves that have been obtained through a simulation where we allowed for chain crossing. The curves are similar to, yet clearly distinguishable from, the curves obtained immediately after the collapse (and up to N^2 time steps later).

It is clear that the collapsed polymer, as created in our simulations, does not resemble the fractal globule. However, despite showing $r^2 \sim g$ and $p_c \sim g^{-3/2}$ it is not in equilibrium either. Since collapsing polymers crumple in a hierarchical fashion but the product appears to be well mixed, this suggests that a fractal globule which has a spatially separated structure on all length scales is not stable on the time scale of the collapse. We therefore expect that it dissolves, presumably through the mixing of its substructures on all length scales within $O(N^{1+2\nu})$ or less time units. To check this idea we study in the following the dynamics of fractal globules. We prepare the fractal starting configuration by hand and then relax the configuration in a poor solvent, thereby maintaining the globular state of the system. We especially ask how long it takes for the fractal state to disappear and whether this process is faster than the polymer collapse presented in the current subsection.

C. Fractal globule dynamics with chain crossing

Our starting configuration here and in Secs. II D and III D is the randomized fractal globule that lives on a FCC lattice, see Sec. II D. The FCC fractal grows by a factor of 8

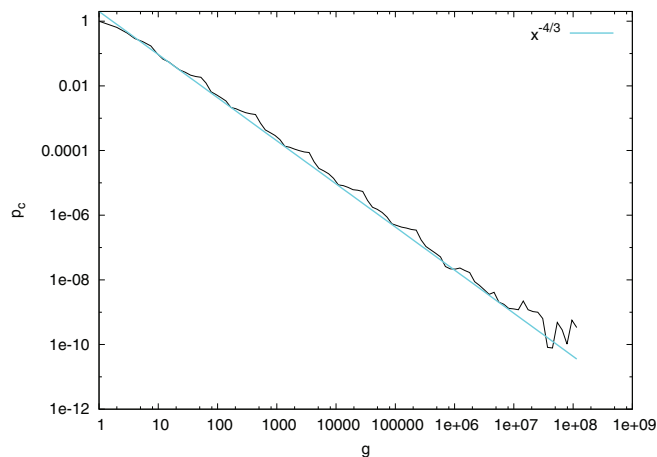


FIG. 5. Contact probability of our fractal globule with smoothing constant $q = 8^{1/11}$ at each step. See text for details.

each generation, or equivalently, a factor of two in each spatial direction.

As discussed in Sec. III A, the contact probability is expected to exhibit power law behavior, namely, $p_c \sim g^{-4/3}$. Instead of plotting $p_c(g)$ directly in a double logarithmic plot, we smoothed the data points over intervals $[g, qg]$, where q is the smoothing constant. Choosing $q = 8^{1/11} \approx 1.21$ we find “bumps” in the p_c plot that are periodic with an interval $\log g = 8$, see Fig. 5. If we choose q to be the growth factor of the fractal, $q = 8$ in our case, these bumps disappear resulting in a smooth curve. As predicted, we find a slope of $-4/3$.

We now let the smooth fractal globule equilibrate with chain crossing allowed but with the self-avoidance constraint still present. In our simulations we accept all proposed chain crossing moves. The effect of chain crossing of the polymer is analogous to the presence of topoisomerase II (topo II) in the nucleus of a cell. Topo II is an enzyme that cuts both strands of a DNA double helix, passes another unbroken double helix through it, and finally reanneals the cut strands. Allowing chain crossing makes the problem easier analytically, because the polymer will essentially behave as a Rouse chain on length scales smaller than the radius of the globule. Moreover, since the polymer does not experience as much topological constraints, the equilibration is also significantly faster.

Because movement is less topologically constrained, we expect for timescales not too short, but before monomers start to feel the constraint of the surface of the globule, that monomers behave as $\langle |r(t) - r(0)| \rangle \sim t^{1/4}$ with a prefactor that is linearly dependent on the concentration of topo II. The exponent $1/4$ is only valid when the monomers have no excluded volume (θ -solvent) or, as here the case, when the excluded volume is screened by other monomers.¹⁷ Since the size of the globule is $N^{1/3}$, it takes $\tau \sim N^{4/3}$ time steps for each monomer to completely renew its position within the globule. As all monomers renew their positions in that timescale, the polymer will be equilibrated within that time. Another way to derive this relation is to realize that an equilibrium globule can be interpreted as $N^{1/3}$ subchains of length $N^{2/3}$ in a globule of size $N^{1/3}$. The Rouse time of each subchain is proportional to the square of its length, i.e., proportional to $N^{4/3}$.

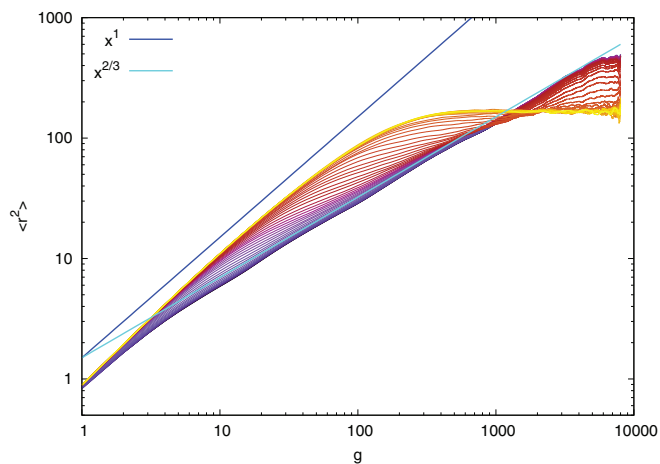


FIG. 6. Equilibration with chain crossing of a $N = 8000$ smooth random FCC fractal. Chain crossing is allowed. This is a mean squared displacement versus the genomic distance $g = |i - j|$ plot. The time starts with the black curve at $t = 0$ and increases exponentially in 48 steps from $t = 1$ to $t = N^2$.

In Figs. 6 and 7 we present the time evolution of the functions $r^2(g)$ and $p_c(g)$ for a chain of polymerization degree $N = 8000$. At the start of the simulation we obviously find the scaling relations of a smooth fractal globule, namely, $r^2 \sim g^{2/3}$ and $p_c \sim g^{-4/3}$. The curves have been taken at times with an exponential distances from each other, $t_i = N^{2i/48}$, and go up to N^2 time units. As can be seen in the plots, the curves already reach a state characterized by $r^2 \sim g$ and $p_c \sim g^{-3/2}$, much before the end of the simulation. Since the equilibration time is proportional to $N^{4/3}$, we expect this state to correspond to the equilibrium molten globule.

As discussed earlier, the state after a polymer collapse shows similar behavior of $r^2(g)$ and $p_c(g)$ but is not in equilibrium. We therefore need a better diagnostic tool that picks up the differences between globules more clearly. Since the main difference between the different structures is expected to be of topological nature, we introduce a quantity for entanglements, the knotting fraction $n_{\min}/n_{\min}^{\text{eq}}$. Here n_{\min} is the av-

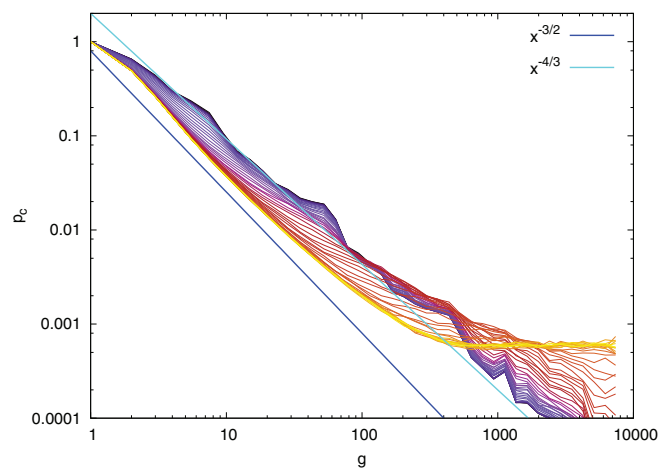


FIG. 7. Equilibration with chain crossing of a $N = 8000$ smooth random FCC fractal. It shows the contact probability as a function of the genomic distance. The time starts with the black curve at $t = 0$ and increases exponentially in 48 steps from $t = 1$ to $t = N^2$.

erage length of the polymer after shrinking it in a Monte Carlo simulation as short as possible without changing its topological state (an approach inspired by the primitive path analysis presented in Ref. 19). The value n_{\min}^{eq} is the measured average of n_{\min} for the equilibrium globule. To determine n_{\min} we place an unbreakable crosslink between the two monomers that are furthest apart along the chain but next to each other in space. This leads to a ring polymer with two dangling ends. Then we run the simulation, but every time step we remove, if possible, one monomer from the complete chain. Also, on a shorter interval (1/2 time step), we attempt to replace the crosslink as to create a larger ring polymer with shorter dangling ends. The simulation ends after $4N/3$ time steps. Note that since the polymer length decreases in time, the number of Monte Carlo moves is actually less than $4N^2/3$.

Since entanglements cannot escape the ring, a point is reached where the ring cannot be made any smaller without changing the topological state of the ring polymer. Thus, the minimal length of the ring is a rough measure for the knot complexity of its initial configuration. Of course, in the time between the start of this simulation and the time that the whole polymer forms a ring, without any dangling ends, entanglements may form as the crosslink is moved changing the topological state of the ring. However, our results suggest that this effect is small.

Figure 8 shows the knotting fraction as a function of time. The plot is consistent with our prediction $\tau \sim N^{4/3}$. Full knotting (and equilibration at the same time) occurs after $\sim N^{4/3}$ time steps, but local knotting (small knots of size $O(1)$) is expected to occur in order 1 time steps because knots are created all along the polymer chain in parallel. The number of local knots at shorter timescales grows proportional to the length of the polymer N , thus reaching a given knot fraction in a constant time. This can be seen by the curves in Fig. 8 shifting to the left as N grows bigger. The fact that the curves do not shift smoothly to the left (for example, the curve with length $N = 4000$ falls on top of the one with $N = 8000$) is due to the fact that we can only create smooth fractals of globular

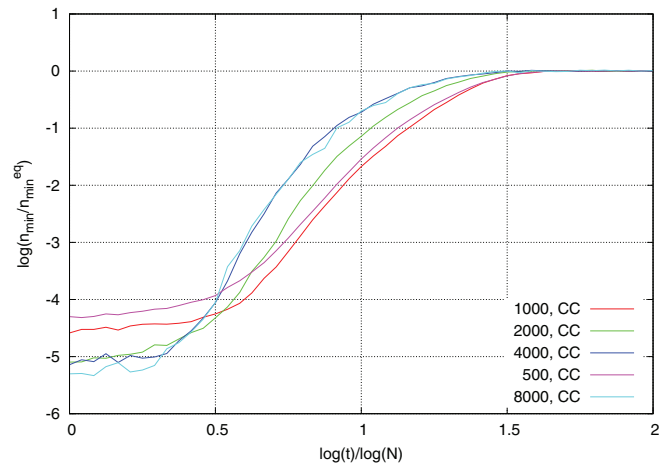


FIG. 8. The knotting fraction $n_{\min}/n_{\min}^{\text{eq}}$ as a function of time. The simulation starts with a fractal globule, and then equilibrates with a self-attraction. The Monte Carlo simulation includes a move that allows two chains to cross each other.

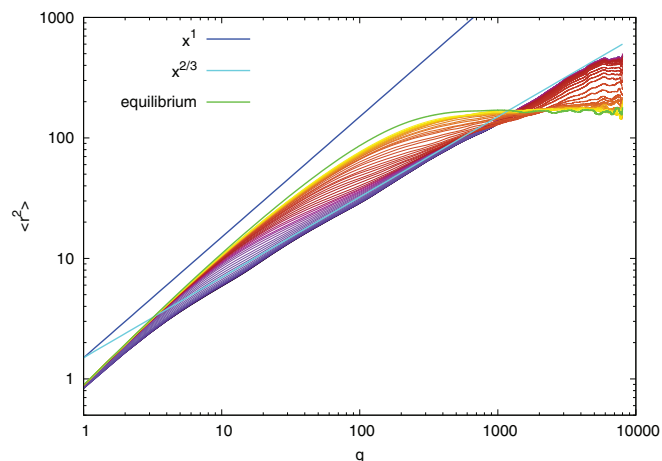


FIG. 9. Equilibration without chain crossing of a $N = 8000$ smooth random FCC fractal. Chain crossing is not allowed in this simulation. This is a mean square displacement versus the genomic distance $g = |i - j|$ plot. The time starts with the black curve at $t = 1$ and increases exponentially in 50 steps to $t = N^2$.

shape for lengths 8^m with m being an integer. The $N = 8000$ chain is created by cutting the $N \approx 32\,000$ to a fourth of its length. This cut polymer has a different shape, more specifically, a higher surface to volume ratio and thus does not knot as quickly as a closer to spherical version of such a fractal.

D. Fractal globule dynamics without chain crossing

The question how long it takes to fully equilibrate a fractal globule without chain crossing (e.g., for DNA in the absence of topo II) is much harder to answer than the previous case. The most straightforward argument is that the globule will only equilibrate through standard reptation, implying an equilibration time $\tau \sim N^3$, see Ref. 1. We cannot simulate chains of sufficient length on that time scale but we show in this section that substantial rearrangement of the fractal globule takes already place on a much shorter time scale.

In Figs. 9 and 10 we present the time evolution of the functions $r^2(g)$ and $p_c(g)$ for a chain of length $N = 8000$. For $t = 0$ we find the scaling relations of a smooth fractal globule, $r^2 \sim g^{2/3}$ and $p_c \sim g^{-4/3}$. As in Figs. 6 and 7 the curves have been taken at times with an exponential distances from each other, $t_i = N^{2i/48}$. Note that within N^2 time steps the smooth fractal globule reaches a state characterized by $r^2 \sim g$ and $p_c \sim g^{-3/2}$. Again, as is the case after the collapse of a polymer (Figs. 3 and 4), we reach a state that appears to be that of the equilibrium molten globule. That we have yet to reach true equilibrium, can be seen by comparing the curves to the equilibrium ones, also shown in Figs. 9 and 10 (green curves). The differences are small but become dramatic when inspecting the time development of the knotting fraction.

In Fig. 11 we present the knotting fraction $n_{\min}/n_{\min}^{\text{eq}}$ of chains of different length as a function of time. The knotting of the chain clearly grows much slower than for a polymer with chain crossing, Fig. 8. However, our plot suggests that substantial knotting already occurs after N^2 time steps, i.e., much shorter than N^3 steps, for all lengths considered (up to $N = 8000$), see Fig. 11. This may be attributed to an extremely

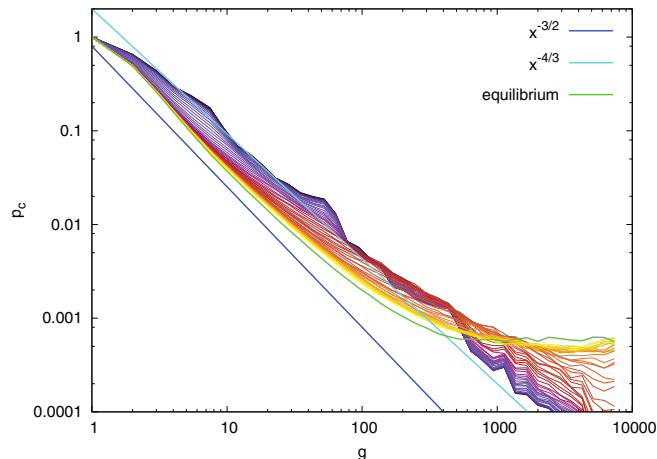


FIG. 10. Equilibration without chain crossing of a $N = 8000$ smooth random FCC fractal. Chain crossing is not allowed in this simulation. Depicted is the contact probability as a function of the genomic distance. The time starts with the black curve at $t = 1$ and increases exponentially in 50 steps to $t = N^2$.

small temporal prefactor, but we speculate here that the polymer can already partially knot itself within a timescale N^2 . Knots are created at the ends of the polymer at a constant rate independent of the length of the polymer. If one such knot is of size $O(1)$ and consists only of a local self-entanglement, it can diffuse along the polymer chain with a diffusion coefficient that is again independent of N . After $O(N^2)$ time steps these knots will have diffused all along the polymer chain, and thus the polymer will be partially knotted with a number of self-entanglements that is proportional to N . Knot-knot “collisions” do not affect this scaling argument since the affected knots can be renumbered after each collision.

To fully equilibrate, local entanglements will have to grow into entanglements of the size of the whole polymer, thereby acquiring a friction proportional to N . This extra factor N suggests that a globule can only fully equilibrate after $\tau \sim N^3$ which in fact scales like the refreshment time of a reptating polymer. Our time series are too short, however, to find conclusive evidence for this prediction.

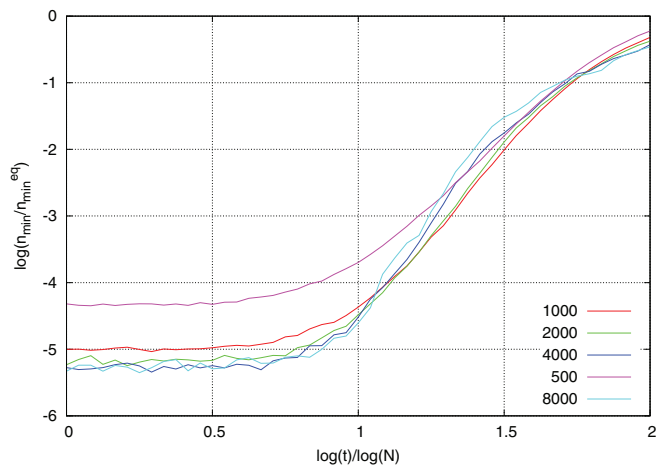


FIG. 11. The knotting fraction $n_{\min}/n_{\min}^{\text{eq}}$ as a function of time. The simulation starts with a fractal globule, and then equilibrates with a self-attraction. Chain crossing is not allowed.

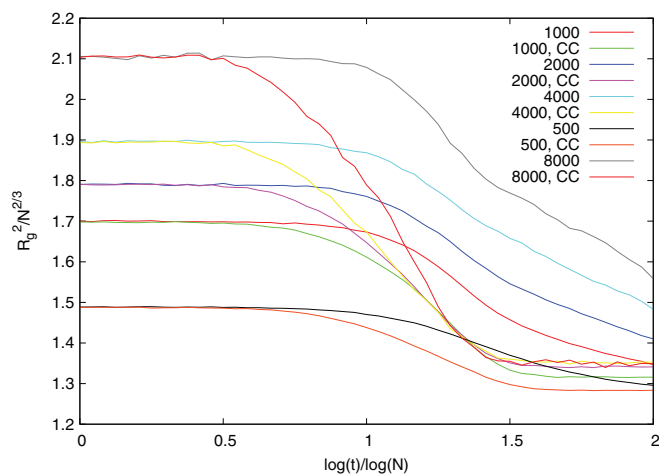


FIG. 12. Final radius of gyration R_g after swelling the globules that have been relaxed for t time steps, either with or without chain crossing moves. Each polymer globule is swelled for $2N$ time steps, before its radius of gyration is measured. The ones with chain crossing are indicated in the plot by CC in the key. Globules with few entanglements will swell much more easily than ones with many of them.

Our algorithm to determine the knot fraction has no direct experimental counterpart. A more physical way to detect entanglements is to reswell a globule by switching off the attraction between the monomers (see also Ref. 9 for a similar approach). This can be realized in an experiment through a change in solvent quality, e.g., by changing the temperature or the ionic strength. In our simulation we simply switch off the attractive interaction and record the size of the chain after $2N$ steps. In Fig. 12 we depict the radius of gyration squared R_g^2 divided by $N^{2/3}$ as a function of $\log(t)/\log(N)$, where t denotes the time the fractal globule had to equilibrate under poor solvent conditions before the swelling phase. Different curves correspond to different chain lengths and to chains that either have been equilibrated with or without chain crossing. Obviously, after we switch off the self-attraction we do not allow for chain crossing anymore.

All the curves share the overall same shape. For very short times t the chain has no time to get entangled and thus swells rapidly after being put into a good solvent. There is no detectable difference between chains that had been equilibrated with or without chain crossing. The same is true for very long times where the chain had enough time to completely entangle. Such equilibrated chains get quickly arrested during swelling due to the entanglements and probably do not grow much beyond their starting size $R_g \sim N^{2/3}$. Our simulation time without chain crossing is unfortunately too short to have reached that state for all cases studied.

In between there is a crossover region where chains swell to an intermediate size within the $2N$ swelling time steps. The location of this crossover is very sensitive to whether the fractal globule had been equilibrated with or without chain crossing. In the former case we expect equilibration within $t \sim N^{4/3}$ and the data for the longest chain $N = 8000$ clearly support this prediction as the curve reaches its equilibrium value around $\log(t)/\log(N) = 4/3$. On the other hand, when chain crossing had been forbidden during the equilibration step the chain has not yet reached full entanglement after

$t \sim N^2$ steps. Equilibration is attained much later, presumably at $t \sim N^3$ that is outside the available simulation time for the longest chains.

IV. DISCUSSION AND CONCLUSION

In this paper we studied the fractal globule, a non-equilibrium polymer state that is characterized by being demixed at all length scales. Its most important property is the absence of entanglements, a property that makes this state one of the prime candidates for the conformations of long eukaryotic DNA inside cell nuclei.^{1,4,9} Our study indicates, however, that the very property of being unentangled also brings about the immediate destruction of the fractal state. In fact, we found that the conformation of a polymer after a collapse shares many features with an equilibrium globule, e.g., it features a monomer-monomer distance that scales like $r^2 \sim g$ for $g < N^{2/3}$ and then level off at a value $r^2 \sim N^{2/3}$. The latter is a clear hallmark that the chain is mixed, even on the largest length scales—unlike the fractal globule state. We observed a similar behavior when starting from a fractal globule configuration: within a time much shorter than the expected N^3 time units, one reaches again such a pseudo-equilibrium state. This can also be seen through inspection by eye of the example configurations shown in Fig. 13. After N time steps the globule is basically still demixed on all length scales, no matter whether we simulate with (upper left) or without chain crossing (upper right). After N^2 time steps the structures are mixed with (lower left) and without chain crossing (lower right).

We speculate that the reason why fractal globules mix so quickly lies in the absence of entanglements allowing mixing of the chain on all length scales without hindrance through entanglements. An example for such a move is shown in Fig. 14 for a Moore curve, a variant of the Hilbert curve. The whole chain consists of four parts that are each folded in the same way. The left and right parts of the square that is occupied by the whole chain are only connected by one strand. The curve can thus be easily opened up in the middle and have the individual parts rotated around, such that a new structure emerges, where large scale rearrangement has taken place. Many similar moves exist allowing an effective mixing of the globule. Obviously the mixing of three-dimensional fractal globules is even easier to achieve. Altogether this suggests that the concept of a well-defined entanglement length¹⁹ might not be useful for such self-similar unentangled conformations. Because of this, the concept of fractal globules might be questionable as well due to the extremely short life time of this configuration.

Theoretical work by Grosberg *et al.*¹ suggested an analogy between the dynamics of fractal globules and the properties of nonconcatenated ring polymers. We do not have any reason to question the observation that rings are demixed,^{2,3} our simulation model has verified this result. However, the present work does not provide evidence supporting the analogy. On the other hand, we cannot exclude the possibility that such an analogy might be useful for describing the dynamics of fractal globules of sizes that are even bigger than the ones presented here.

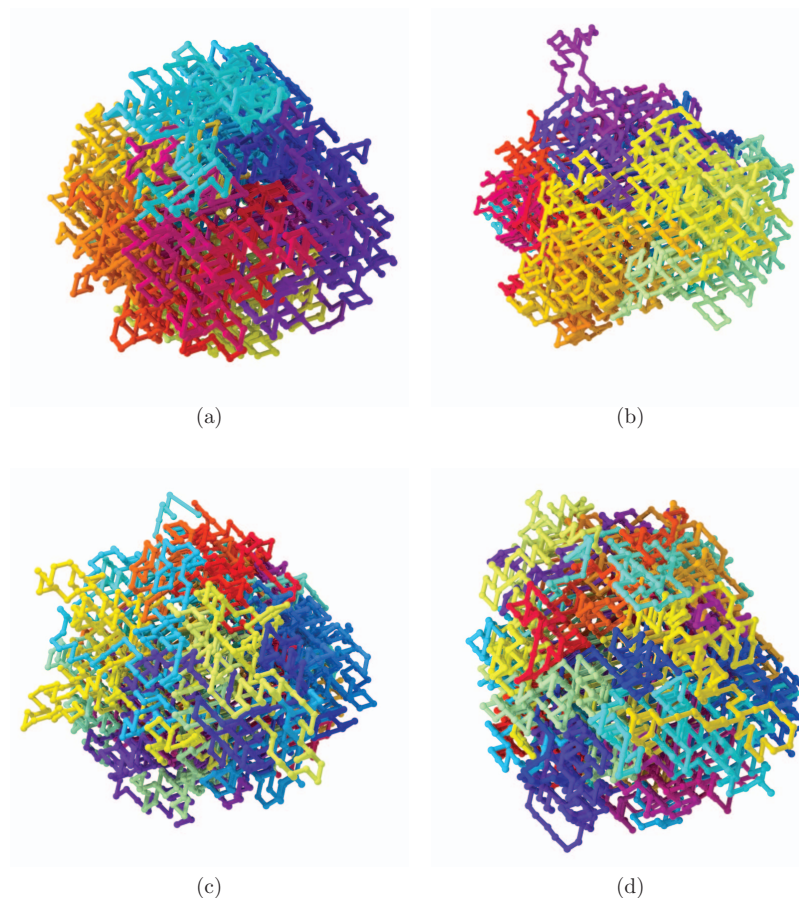


FIG. 13. A polymer of length 4000 in different states. On the left the simulation is done without chain crossing, while polymers on the right are simulated with chain crossing. The polymers on top are shown after letting the FCC fractal equilibrate for N time steps. The two pictures below are equilibrated for N^2 time steps. The renders are made using the pov-ray package.

Nevertheless, in the simulations presented in Ref. 9 fractal globules have been clearly observed that had been induced by a polymer collapse. These states were clearly self-similar and demixed on all length scales. We speculate that the main reason for the disparity between our respective conclusions is that our simulation time is much longer. Pictures taken of our own globules at around N time steps show a lot of similarities to theirs. The fact that they found a crumpled globule directly after the collapse could possibly be explained by the speed of their collapse, which is much higher (and we would argue unnaturally high) than in our case.

Another question in this context concerns the exponent characterizing the decay of the contact probability with distance. Mathematical space filling fractals typically show a $-4/3$ slope but the simulated fractal globule of Ref. 9 suggests $p_c(g) \sim g^{-1}$. We can compare this with the time development

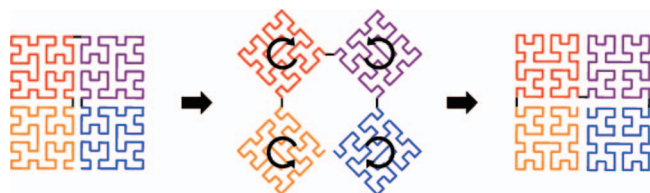


FIG. 14. One of many possible mixing moves for a Moore curve, a variant of the Hilbert curve.

of $p_c(g)$ that we found when relaxing a fractal globule without chain crossing, see Fig. 10. Shortly after starting relaxation – at about N time steps – the contact probability shows at intermediate length scales roughly a -1 power law as a function of g . If we assume that this intermediate state is an interdigitating fractal, the structure on the largest length scales had at least to move by an amount proportional to $N^{1/3}$, because according to its definition the interdigitating depth needs to scale as $g^{1/3}$ for a chain segment of length g . This would, however, take at least $N^{4/3}$ time steps (via Rouse dynamics in the absence of entanglements) and is thus too slow.

Instead we suggest that the -1 slope we found is in fact an artifact of a relatively broad crossover between Gaussian chain behavior on short length scales ($p_c \sim g^{-3/2}$) and still fractal behavior at long length scales ($p_c \sim g^{-4/3}$). At first sight this might seem counterintuitive because -1 is less negative than both $-4/3$ and $-3/2$. The key here is that the two curves do not connect in one crossover point, but in a “zigzag” fashion, see Fig. 15. It is not hard to see why this should be the case. We find that both the original fractal globule and the newly appearing Gaussian regime show approximately the same prefactor in their contact probability power law (because $p_c(1) = 1$ by definition). In addition to this, the prefactor of the still fractal part (large g) increases over time due to the roughening of the surface. Thus, it is easy to see that the two curves will not connect in a point, but instead will have to

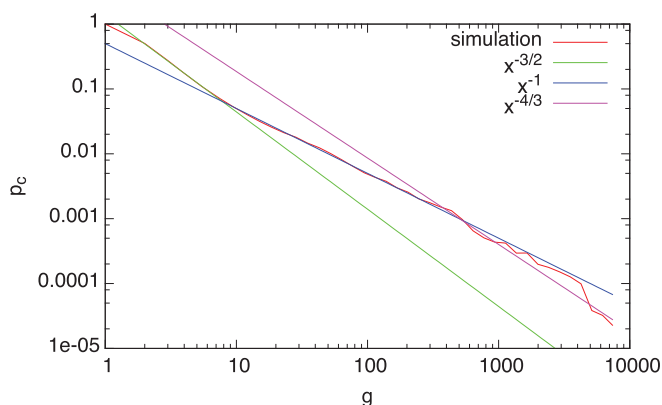


FIG. 15. Contact probability p_c as a function of genomic distance g at $t = N^{0.92}$, for a polymer of length $N = 8000$. The lines indicate the perceived “zigzag” as elaborated in the main text. The full time development is shown in Fig. 7.

form a “zigzag” like structure. In our simulations we find an approximate -1 slope, but we are unsure whether this is due to the limited size of the fractal or not.

In our simulations we found that fractal globules are rather unstable and quickly move to the pseudo-equilibrium globule, an ensemble of states that is very hard to discern from the equilibrium globule with regard to both the contact probability and the monomer-monomer distance. However, we identify this class from the equilibrium globule by the amount of self-entanglement that, e.g., manifests itself in a much faster swelling behavior when the globule is put into a good solvent.

Interestingly in the context of chromatin the experimentally accessible quantities happen to be the contact probability (obtained through chromatin conformation capture) and the monomer-monomer distance (obtained through FISH). The latter is less conclusive but conformation captures indicates a decay in the contact probability not substantially faster than g^{-1} . If we insist on entanglement-free DNA conformations, this excludes both smooth fractal globules (slope $-4/3$) and pseudo equilibrium globules (slope $-3/2$). On the other hand, we have not seen any numerical evidence for the existence of interdigitating globules.

To conclude, our simulations have not given any evidence that collapsed linear polymers show $p_c(g) \sim g^{-1}$. This suggests that in order to build large-scale models of interphase chromatin one might have to move away from models of linear polymer chains to, e.g., solutions of rings^{2,20} or one has to introduce suitable cross-linking between different parts of a linear polymer chain.

ACKNOWLEDGMENTS

We would like to thank Marc Emanuel, Jean-François Joanny, and Jean-Charles Walter for discussions. This work is part of the research programme of the Foundation for Fundamental Research on Matter (FOM), which is financially supported by the Netherlands Organisation for Scientific Research (NWO).

APPENDIX: MORE ELABORATE DERIVATION OF CONTACT PROBABILITY FOR FRACTAL GLOBULES

To derive the contact probability of a “fractal globule”, we first have to define exactly what we mean by that term. Here, we define our fractal object as one where at each length scale the contacts between the 2^d neighboring smaller parts “look” the same: the fraction f_I of the surface in between them divided by the total surface of the individual parts (without taking the contact between the parts into consideration) is equal for all length scales. The last assumption is that the blocks build themselves in a fractal way: 2^d consecutive blocks are ordered inside a larger $2 \times 2 \times 2$ block (in the case of 3 dimensions). The effect of this is that the surface of a large blob can be fractal with a dimension higher than $d - 1$. We define S_1 as the surface of the elementary building block where the globule starts to be fractal.

Using these definitions, we now derive the contact probability, without even needing to know the fractal dimension of the globule, which is constrained, though not necessarily uniquely determined, by the value of f_I . Since we are not interested here in these constraints, we will refrain from deriving them. Our derivation here is neither limited to polymers, though with the ordering constraint of the blocks, assuming connected bonds is a rather loose constraint.

Since blocks are connected to each other through their surface that is determined by the surfaces of the smaller blocks it constitutes of, we first derive the surface of a block of g elementary blocks. The first new surface area S_{2^d} is a function of the surface of the elementary blocks and the internal surface fraction f_I :

$$S_{2^d} = (1 - f_I)S_1 2^d. \quad (\text{A1})$$

Thus we get for arbitrary $g = (2^d)^k$:

$$S_g = (1 - f_I)^k S_1 g. \quad (\text{A2})$$

Using that $k = \log(g)/\log(2^d)$, we find that

$$S_g = (1 - f_I)^{\log(g)/\log(2^d)} g S_1 = g^{1 + \frac{1}{d} \frac{\log(1-f_I)}{\log(2)}} S_1. \quad (\text{A3})$$

For simplicity of the argument we only find the contact probability of monomers with a block of g monomers, at least $g2^{-d}$ monomers apart, where the last condition ensures that monomers are in separate sub-blocks. Thus, the resulting contact probability $p_c(g)$ is actually a (weighted) average over the interval $[g2^{-d}, g]$. Since we are not interested in a complete explicit formula, but more in scaling and the dependence on f_I without caring too much about small corrections, this assumption suffices for us.

The total surface of the sub-blocks is given by $S_g/(1 - f_I)$, which follows readily from their respective definitions. Then the internal surface of all sub-blocks is given by $M_g = S_g f_I / (1 - f_I)$. To obtain the contact probability, we find the total number of possible contacts, that can be found between monomers that are within a g block, more than $g2^{-d}$ apart, which is given by $Q_g = 1/2(1 - 2^{-d})g^2$. Thus we find for the

contact probability

$$p_c(g) = M_g/Q_g = \frac{2f_I S_g}{(1-f_I)(1-2^{-d})g^2} \\ = \frac{2f_I S_1}{(1-f_I)(1-2^{-d})} g^{-1+\frac{1}{d}\frac{\log(1-f_I)}{\log(2)}}. \quad (\text{A4})$$

Thus for the case of a smooth fractal, we have $f_I = 0.5$, and we get $p_c \sim g^{-1-1/d}$, which is the same as given in the main text. Since this is the highest possible value of f_I , and we can get anything down to $f_I = 0$, we find for the possible values of the exponent: $-1 > \beta \geq -4/3$. Note however that if f_I goes to 0, the prefactor also goes to 0. Thus, getting exactly a -1 law is impossible with our assumptions, though we can approach it arbitrarily close, with an increasingly small prefactor.

¹A. Y. Grosberg, S. K. Nechaev, and E. I. Shakhnovich, "The role of topological constraints in the kinetics of collapse of macromolecules," *J. Phys. (France)* **49**, 2095–2100 (1988).

²J. D. Halverson, W. B. Lee, G. S. Grest, A. Y. Grosberg, and K. Kremer, "Molecular dynamics simulation study of nonconcatenated ring polymers in a melt. I. Statics," *J. Chem. Phys.* **134**, 204904-1–204904-13 (2011).

³T. Vettorel, A. Y. Grosberg, and K. Kremer, "Statistics of polymer rings in the melt: A numerical simulation study," *Phys. Biol.* **6**, 025013 (2009).

⁴A. Grosberg, Y. Rabin, S. Havlin, and A. Neer, "Crumpled globule model of the three-dimensional structure of DNA," *Europhys. Lett.* **23**, 373–378 (1993).

⁵G. van den Engh, R. Sachs, and B. J. Trask, "Estimating genomic distance from DNA sequence location in cell nuclei by a random walk model," *Science* **257**, 1410–1412 (1992).

⁶R. K. Sachs, G. van den Engh, B. Trask, H. Yokota, and J. E. Hearst, "A random-walk/giant-loop model for interphase chromosomes," *Proc. Natl. Acad. Sci. U.S.A.* **92**, 2710–2714 (1995).

⁷J. Mateos-Langerak *et al.*, "Spatially confined folding of chromatin in the interphase nucleus," *Proc. Natl. Acad. Sci. U.S.A.* **106**, 3812–3817 (2009).

⁸M. Emanuel, N. H. Radja, A. Henriksson, and H. Schiessel, "The physics behind the larger scale organization of DNA in eukaryotes," *Phys. Biol.* **6**, 025008-1–025008-11 (2009).

⁹E. Liebermann-Aiden *et al.*, "Comprehensive mapping of long-range interactions reveals folding principles of the human genome," *Science* **326**, 289–293 (2009).

¹⁰L. A. Mirny, "The fractal globule as a model of chromatin architecture in the cell," *Chromosome Res.* **19**, 37–51 (2011).

¹¹C. F. Abrams, N.-K. Lee, and S. P. Obukhov, "Collapse dynamics of a polymer chain: Theory and simulation," *Europhys. Lett.* **59**, 391–397 (2002).

¹²A. Lappala and E. Terentjev, "'Raindrop' coalescence of polymer chains during coil-globule transition," *Macromolecules* **46**, 1239–1247 (2013).

¹³M. Bohn, D. W. Heermann, and R. van Driel, "Random loop model for long polymers," *Phys. Rev. E* **76**, 051805 (2007).

¹⁴M. Rubinstein, "Discretized model of entangled-polymer dynamics," *Phys. Rev. Lett.* **59**, 1946 (1987).

¹⁵D. Panja and G. T. Barkema, "Rouse modes of self-avoiding flexible polymers," *J. Chem. Phys.* **131**, 154903 (2009).

¹⁶M. Baiesi, G. T. Barkema, E. Carlon, and D. Panja, "Unwinding dynamics of double-stranded polymers," *J. Chem. Phys.* **133**, 154907 (2010).

¹⁷R. Lua, A. L. Borovinskiy, and A. Y. Grosberg, "Fractal and statistical properties of large compact polymers: A computational study," *Polymer* **45**, 717–731 (2004).

¹⁸P. G. de Gennes, "Dynamics of entangled polymer solutions. I. The Rouse model," *Macromolecules* **9**, 587–593 (1976).

¹⁹R. Everaers, S. K. Sukumaran, G. S. Grest, C. Svaneborg, A. Sivasubramanian, and K. Kremer, "Rheology and microscopic topology of entangled polymeric liquids," *Science* **303**, 823–826 (2004).

²⁰A. Rosa and R. Everaers, "Structure and dynamics of interphase chromosomes," *PLOS Comput. Biol.* **4**, e1000153 (2008).